Proceedings of the ASME 2010 3rd Joint US-European Fluids Engineering Summer Meeting and 8th International Conference on Nanochannels, Microchannels, and Minichannels
FEDSM-ICNMM2010
August 1-5, 2010, Montreal, Canada

FEDSM-ICNMM2010-30483

SPANWISE CORRELATION OF SURFACE PRESSURE FLUCTUATIONS IN HEAT EXCHANGER TUBE ARRAYS

John Mahon
School of Engineering
Trinity College Dublin
Dublin, Ireland
Email: mahonjp@tcd.ie

Paul Cheeran
School of Engineering
Trinity College Dublin
Dublin, Ireland
Email: cheeranp@tcd.ie

Craig Meskell *
School of Engineering
Trinity College Dublin
Dublin, Ireland
Email: cmeskell@tcd.ie

ABSTRACT

An experimental study of the surface spanwise pressure on a cylinder in the third row of two normal triangular tube arrays (P/d=1.32 and 1.58) with air cross flow has been conducted. A range of flow velocities were examined. The correlation of surface pressure fluctuations due to various vibration excitation mechanisms along the span of heat exchanger tubes has been assessed. The turbulent buffeting is found to be uncorrelated along the span which is consistent with generally accepted assumptions in previous studies. Vortex shedding and acoustic resonances were well correlated along the span of the cylinder, with correlations lengths approaching the entire length of the cylinder. Jet switching was observed in the pitch ratio of 1.58 and was found to be correlated along the cylinder, although the spatial behaviour is complex. This result suggests that the excitation force used in fretting wear models may need to be updated to include jet switching in the calculation.

NOMENCLATURE

d	Tube diameter
l	Tube length
f_v	Vortex shedding frequency
P	Pitch
P/d	Pitch ratio
R	Correlation coefficient
Re	Reynolds number
S	Strouhal number
U	Free stream flow velocity
U_g	Gap velocity
z	Co-ordinate in tube axis direction
θ	Position angle

INTRODUCTION

Heat exchanger tube arrays are susceptible to flow-induced vibrations which often result in component failure and loss of revenue. Turbulent buffeting and vortex shedding are among the various excitation mechanisms which cause flow-induced vibrations.

The random turbulent buffeting forces acting on a tube have been measured by several researchers in a variety of array geometries and so the typical spectral distribution of the excitation is well established. In order to apply this excitation spectrum to the entire tube length an assumption must be made regarding the correlation of these forces along the span of the tube. Axisa *et al.* (1) and others have shown that if this correlation length is much smaller than the overall tube length, then correlation length

*Address all correspondence to this author.

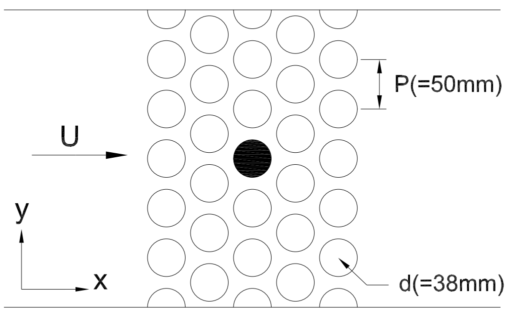

FIGURE 1. Test section schematic, P/d=1.32

is largely irrelevant. They have reasoned that the correlation length is of the order of the tube diameter. However, this is based on relatively sparse experimental data. Batham (2) presented data for the correlation length for a single cylinder. Romberg & Popp (3) conducted a series of tests examining the correlation length and coefficient for a number of tube arrays however only limited data was presented. Nonetheless, a re-examination of this issue has been prompted by the extension of life time of these assemblies coupled with the advent of detailed unsteady flow simulations which require experimental validation.

EXPERIMENTAL SETUP

The experimental facility consists of a draw-down wind tunnel which has a tube array in the test section having a length of 750mm and a cross-section of 300mm x 300mm. In this study, two five row normal triangular tube arrays with pitch ratios of 1.32 and 1.58 were investigated. The diameter of tubes used is 38mm. A schematic of the test-section is shown in Fig. 1.

The free stream velocity in the test section was measured by a pitot-static tube installed upstream of the tube array connected to a Furness Control micromanometer (model FC015). The flow velocities in the test section ranged from 2 to 14m/s with a free stream turbulence intensity of less than 1%. The tubes in the array are rigidly fixed, except for one tube which will be referred to as the instrumented cylinder. The instrumented cylinder has 27 pressure taps of 1mm diameter along its span and are located a distance of 9mm apart. Holes of 1.59mm diameter were drilled along the span on a hollow brass cylinder and brass tubing of 1.59mm outer diameter and 1mm inner diameter was fit into these holes. Air tightness was secured by brazing the connection. It was also ensured that the pressure tap is smooth and burr-free with accurate diameter. The brass tubing from the 27 pressure taps were then taken out through the bottom of the cylinder through a push fit base with a suitable aperture in its center. A solid cap was push fit to hollow brass cylinder was adhered using araldite epoxy resin. The length of the instrumented cylinder was 298mm in the test section. The instrumented cylinder was mounted on a bi-directional traverse, though static displacements were not applied to the cylinder in this study. A collar placed in between the support and the instrumented cylinder aided in rotation of the cylinder to take measurements at different angles with respect to the flow. A schematic of the pressure tap cylinder is shown in Fig. 2.

The instrumented cylinder was connected to pressure transducers using short lengths of silicone tubing with internal diameter 2mm. Each pressure tap was monitored with a differential pressure transducer (Honeywell 164PC01D37). The other port of the pressure transducer was vented to the atmosphere and so in effect gauge pressure was measured. The signal from pressure transducers were acquired using an NI 8 channel, 24 bit data acquisition frame. Each channel was simultaneously sampled and automatically low passed filtered to avoid aliasing. Additional information regarding the experimental setup can be found in (4).

TABLE 1. Velocities and Reynolds numbers tested

	P/d=1.32		P/d=1.58	
U (m/s)	U_g (m/s)	Re $(\times 10^4)$	U_g	Re $(\times 10^4)$
2	8.3	2.23	-	-
3	12.5	3.34	8.2	2.19
4	16.7	4.46	10.9	2.92
5	20.8	5.58	13.6	3.65
6	25.0	6.70	16.4	4.38
7	29.2	7.82	19.1	5.12
8	33.3	8.93	21.8	5.85
9	37.5	10.05	24.5	6.58
10	41.7	11.16	27.3	7.31
11	-	-	30.0	8.04
12	-	-	32.7	8.77
13	-	-	35.4	9.50
14	-	-	38.2	10.23

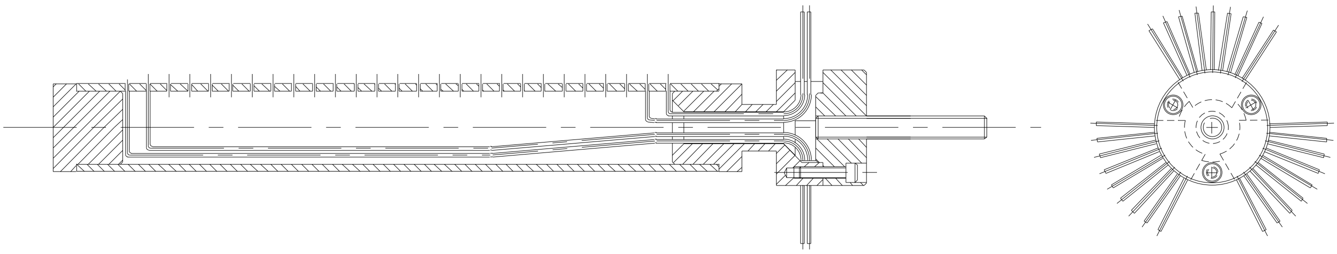

FIGURE 2. Schematic of the pressure tap tube

RESULTS

Tests were conducted for two five row normal triangular tube arrays with pitch ratios of 1.32 and 1.58 with free stream flow velocity ranges of 2-10m/s and 3-14m/s, respectively. The velocities and Reynolds number of the tests are given in Table 1. Note that the Reynolds numbers presented are based on the gap velocities and tube diameter. Twenty seven surface pressure measurements along the length of the cylinder (in the center of the third row) were acquired simultaneously for a duration of 40 seconds at a sample frequency of 3072Hz. The location along the span of the cylinder is denoted by "z" and is zero at the center of the cylinder with positive values on the upper half of the cylinder and negative values on the lower half of the cylinder. Tests were conducted at position angles from 0^o to 180^o at intervals of 10^o for the pitch ratio of 1.32. For P/d=1.58, tests were conducted from 0^o to 350^o at intervals of 10^o. See Fig. 3 for a schematic of the tube position angle. Results on circumferential pressure measurements with static tube displacement for the two arrays under investigation in this study can be found in Mahon & Meskell (4).

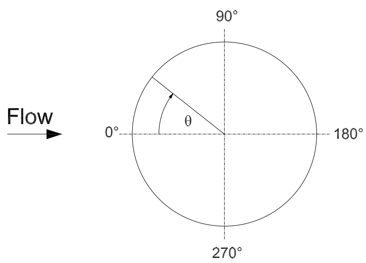

FIGURE 3. Schematic of position angle

Validation of the test setup

In the first instance the experimental setup was validated by comparing the Strouhal numbers for both tube arrays under investigation in this study with Strouhal number data in the literature. The Strouhal number was defined as

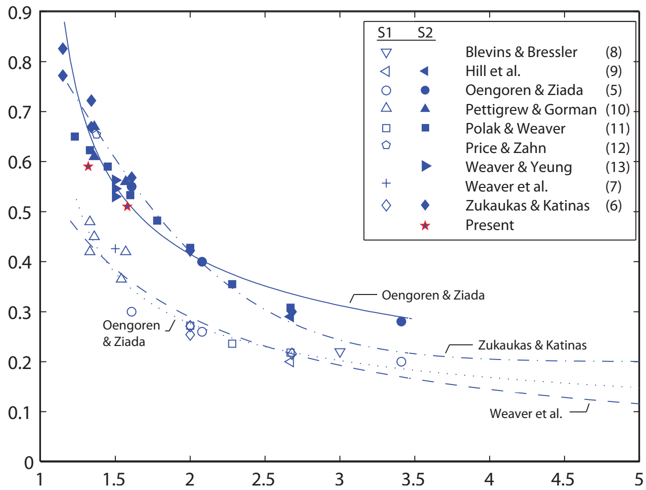

FIGURE 4. Strouhal number distributions of flow periodicities in normal triangular tube arrays as functions of the spacing ratio.

$$S = \frac{fd}{U_g} \tag{1}$$

Oengoren & Ziada (5) collated the Strouhal number data for normal triangular tube arrays for a range of pitch ratios. They reported three vorticity shedding components. A low frequency component, f_{v1}, associated with alternate vortex shedding from the rear rows, a high frequency component, f_{v2} due to alternate vortex shedding from the front rows and a third shedding frequency (f_{v2} - f_{v1}) due to the non-linear interaction between f_{v1} f_{v2}. They plot the available Strouhal number data on a single figure. Using a least squares approximation, they deduced the following empirical forms; S_1 and S_2 for f_{v1} and f_{v2} components, respectively.

$$S_1 = \frac{1}{3.62(X_p-1)^{0.45}}, \quad S_2 = \frac{1}{2.41(X_p-1)^{0.41}} \tag{2}$$

Fig. 4 plots the available Strouhal number data, empirical forms deduced by Oengoren & Ziada as well as the relationship Zukauskas & Katinas (6) obtained for the f_{v2} component of vortex shedding and the relationship Weaver *et al.* (7) predicts the f_{v1} component.

Strouhal numbers of 0.59 and 0.51 were calculated for the pitch ratios of 1.32 and 1.58, respectively. These values are also shown in Fig. 4 and compare well with the experimental data (f_{v2} component) presented in the literature (5) and the empirical expressions of Oengoren & Ziada and Zukauskas & Katinas. There are slight differences observed which are attributed to the differences in the Reynolds numbers tested. Nonetheless, the comparison with the results was satisfactory, demonstrating the integrity of the setup.

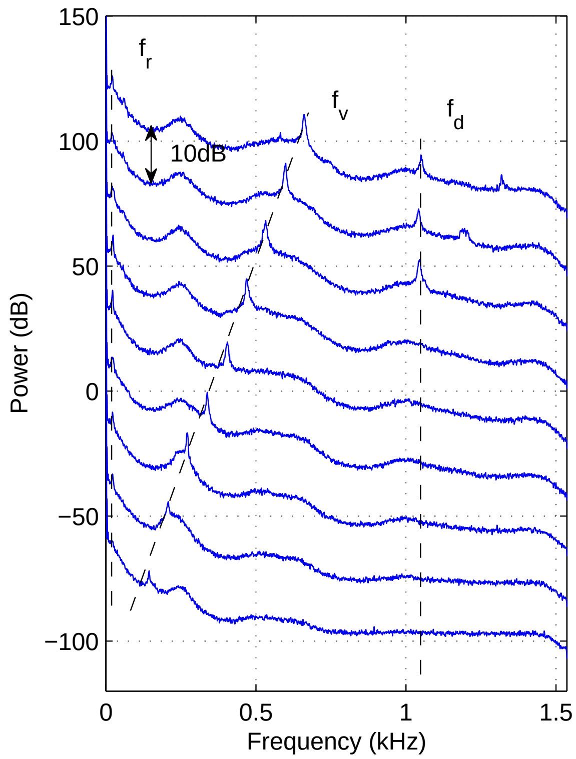

FIGURE 5. Spectrum of pressure signal; P/d=1.32, θ=20^o, z/d=0

Pitch ratio 1.32

A typical spectrum of the pressure signal at θ=20^o for the pitch ratio of 1.32 at different flow velocities is shown in Fig. 5. It was found to have a few characteristic peaks. Room acoustic resonance is shown by f_r which is constant at about 24Hz for all flow velocities. Vortex shedding frequency is shown by f_v which increases linearly with velocity and has a corresponding Strouhal number of 0.59 as discussed above. The duct acoustic resonance (second mode) at approximately 1050Hz is denoted by f_d and this is observed at higher flow velocities (from U_g=33.3m/s). At this velocity the vortex shedding frequency occurs at 530Hz, which is close to the first mode of the duct acoustic resonance frequency. Flow acoustic resonance is seen when the second duct mode frequency coincides with the vortex shedding.

However a lock-in of the vortex shedding frequency with the acoustic resonance frequency of the duct is not observed. If a lock-in had occurred, the vortex shedding frequency would have been synchronized with the duct acoustic resonance frequency over a range of velocities higher than the critical gap velocity of 33.3m/s. This means f_v would have been the same for a velocity range, within which the sound pressure level increases rapidly to a very high value, before coming out of the lock-in. Neither a constant vortex shedding frequency nor a rapid increase in sound level was observed in this case. Hence, acoustic resonance of the duct was triggered even though a lock-in of vortex shedding with the acoustic resonance did not occur. The second harmonic of the vortex shedding frequencies are observed at high flow velocities of 37.5m/s and 41.7m/s.

The spanwise coherence for P/d=1.32 at different angles and velocity is given in Fig. 6. A vortex shedding flow periodicity corresponding to a Strouhal number of approximately 0.59 was observed. For low flow velocities, vortex shedding is found to have low coherence along the span of the cylinder. The coherence is low at the front of the cylinder. It increases until the flow reaches 60^o and gradually decreases until 90^o, suggesting flow separation and the formation of vortices between these angles. After 90^o, the coherence of the vortex shedding frequency reduces further. This trend continues as the position angle tends towards 120^o. At a position angle of 120^o the coherence at the vortex shedding frequency is below the level experienced at the front of the cylinder.

As the flow velocity is increased, it is observed that the vortex shedding frequency is more coherent along the span of the cylinder. Similar to results presented for the lower flow velocities tested, the coherence is low at a position angle of 0^o and increases as flow is convected around the cylinder until the position angle of 60^o is reached. Thereafter, the coherence decreases again as the position angle tends towards the rear of the cylinder. The drop in coherence after 60^o could be due to shedding of vortices from the surface of the cylinder.

Other peaks noted in the coherence plots are attributed to room and duct acoustic resonance. A constant peak along the entire span at 24Hz is observed for most flow velocities and position angles tested. The room and duct resonance frequencies behave in a different manner to vortex shedding frequency. In general, the spanwise coherence of room resonance increases with flow velocity. This is not surprising given there is an increased

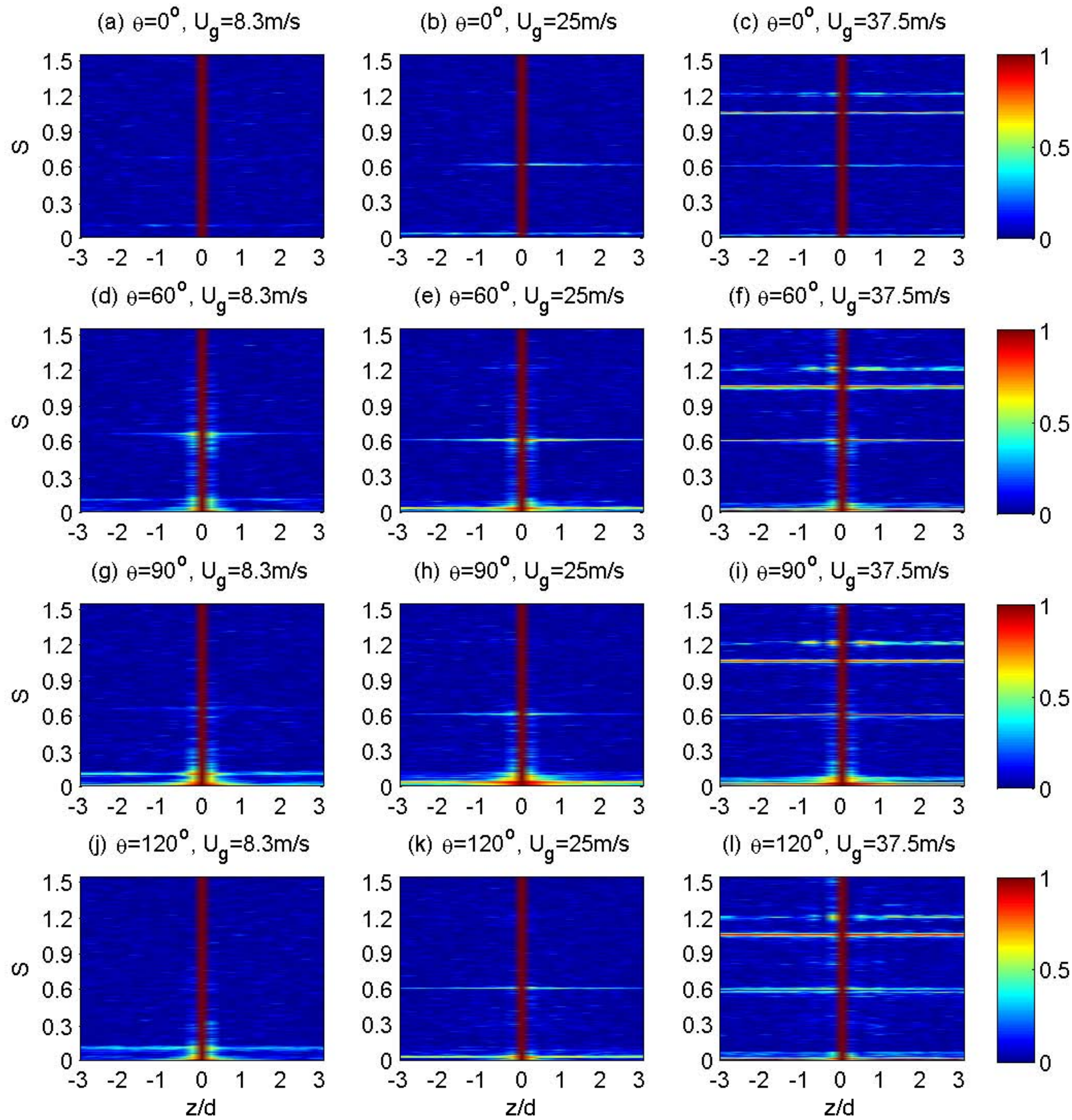

FIGURE 6. Spanwise coherence at different angular positions for P/d=1.32

energy input into the room as the flow velocity is increased. Two duct acoustic modes were observed. The first duct acoustic mode (580Hz) appears at the medium velocity ranges tested. The second duct acoustic mode (1050Hz) as discussed earlier is excited by the vortex shedding and does not occur until higher flow velocities. The first acoustic mode produced less energy than that of the second acoustic mode. It was also observed that as the position angle θ increases, both the room and duct (second mode) resonances increase. At the rear of the cylinder the second acoustic mode of the duct is also observed.

Correlation along the span of the cylinder was found to be very high. This is not surprising given the presence of vortex shedding and the two other peaks, which are highly coherent along the span and hence these would have a significant influence on the correlation coefficient and would result in a high correlation coefficient close to the maximum value of 1 along the entire span. To observe the spanwise correlation due to other flow features, the three known elements viz. vortex shedding frequencies at different flow velocity, room acoustic mode at 24Hz and duct acoustic modes at 580 and 1050Hz, were filtered out from the measured signal. When these components were removed the correlation reduced (see Fig. 7). However, the correlation is still too high. The correlation was found to be higher than in the case of P/d=1.58 and continuously increasing as angle θ increases. Thus, a reliable estimate of correlation length for turbulent buffeting has not been obtained for this tube array.

Another feature of the spanwise correlation for this tube array was found to be the change in correlation with velocity. In general, the spanwise correlation increased as velocity increased reaching constant values at higher flow velocities (See Fig. 8). Fig. 9 demonstrates a different behaviour at the front of the cylinder, were the position angle θ is small. In this case, the correlation coefficient is found to be very small, irrespective of the flow velocity. The very low spanwise correlation at the front of the cylinder which is evident at all flow velocities could suggest the presence of uncorrelated turbulent buffeting forces. However, as the flow progresses around the cylinder, some other mechanisms come into play which increase the correlation to relatively high values and these mechanisms tend to vary with flow velocity. In the case of the pitch ratio of 1.32, further data analysis is required to remove narrowband and deterministic components in the data, particularly at low frequencies.

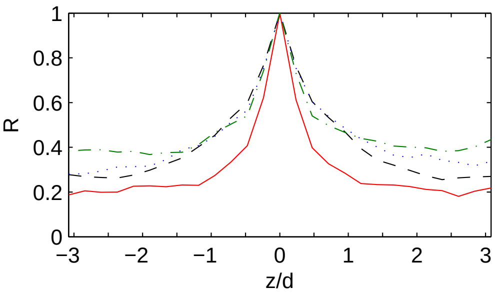

FIGURE 7. Spanwise correlation; P/d=1.32, θ=120^o; —, U_g=8.3m/s; – –, U_g=20.8m/s; ···, U_g=29.2m/s; – · –, U_g=41.7m/s

Pitch ratio 1.58

The coherence along the span of the instrumented cylinder for the tube array with P/d= 1.58 is given in Fig. 10. It was observed that the vortex shedding peak corresponding to Strouhal number of 0.51 has a high coherence along the span. The room acoustic mode at 24Hz had a high coherence for most of the flow velocities and position angles tested. It is also apparent that the second acoustic mode of the duct at 1050Hz is highly

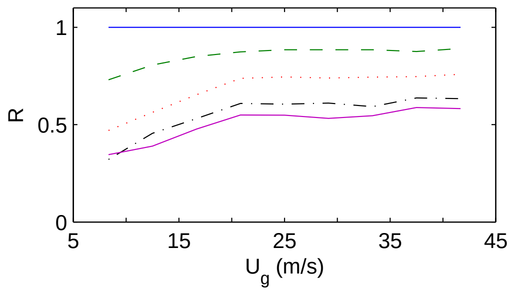

FIGURE 8. Spanwise correlation at different velocities; P/d=1.32, θ=90^o; —, z/d=0; – –, z/d=0.24; ···, z/d=0.71; – · –, z/d=1.66; —, z/d=3.08

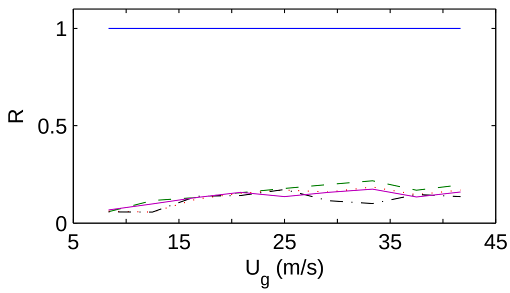

FIGURE 9. Spanwise correlation at different velocities; P/d=1.32, θ=0^o; —, z/d=0; – –, z/d=0.24; ···, z/d=0.71; – · –, z/d=1.66; —, z/d=3.08

coherent along the length of the cylinder at high flow velocities. In Fig. 10 for U_g=34.5m/s, high coherence is observed at a frequency slightly above the vortex shedding frequency (≈530Hz) and this is the first acoustic mode of the duct (580Hz).

Vortex shedding frequencies at different flow velocity, room acoustic mode at 24Hz and duct acoustic mode at 1050Hz, were filtered out from the measured signals as before. This enabled the spanwise correlation due to other features of the flow to be measured. The correlation could now be related to random turbulent buffeting forces or jet switching. The spanwise correlation of the pressure signal at different flow velocities and different angles of flow is shown in Fig. 11 and Fig. 12. The correlation length is found to be less than one diameter at all flow velocities.

The correlation does not vary much with change in flow velocity. This strongly suggests the presence of random turbulent forces, which do not depend on flow velocities. The minimum correlation was observed at θ=0^o. As the flow moves towards the rear of the cylinder i.e. increasing θ, the correlation increases slightly, but not to a large extent. Hence the presence of uncorrelated turbulent buffeting forces has been verified. This is in agreement with the assumption of very low correlation length, made in previous studies (Axisa *et al.* (1), Pettigrew & Taylor (14)).

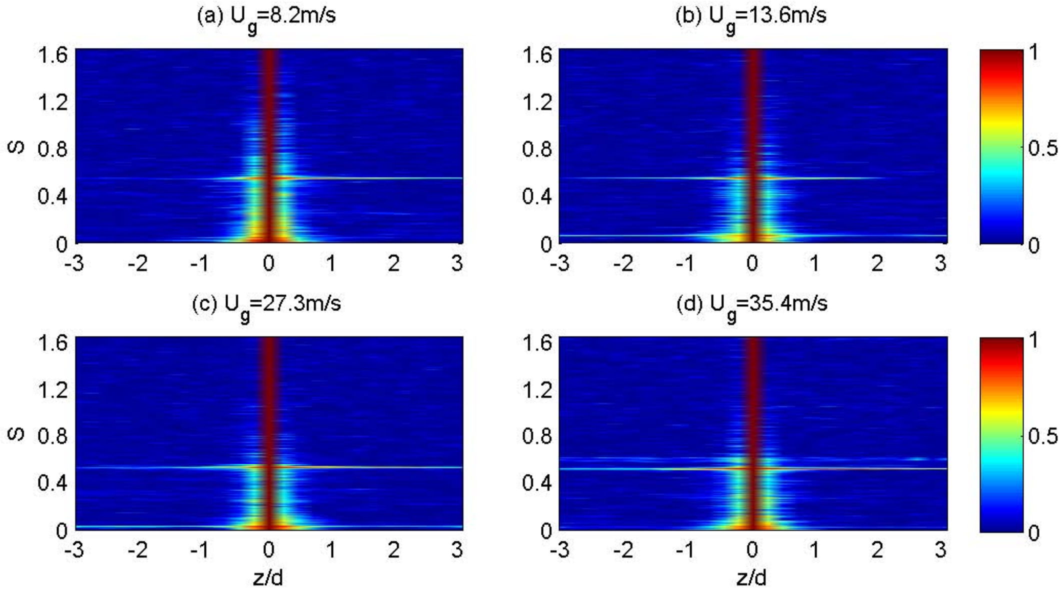

FIGURE 10. Spanwise coherence at a range of flow velocities; P/d=1.58, θ=90^o

Jet switching

In Mahon & Meskell (4), the authors measured the circumferential pressure distribution at the mid span for the normal triangular array with a pitch ratio of 1.58. Large asymmetry in the mean pressure distribution was observed. The asymmetric pressure distribution was investigated and the asymmetry was attributed to bi-modal jet switching. The time resolved lift and drag forces were calculated and large changes in the lift forces were observed due to jet switching.

In the current study, jet switching was also observed along the whole length of the tube. Fig. 13 shows a histogram of pressure signal at $\theta = 250^o$ and at a flow velocity of 7m/s at spanwise positions of z/d=1.66, z/d=0.47, z/d=-1.89 and z/d=-2.61. It is clear that there is a bi-modal flow behaviour and this occurs along the length of the cylinder. The question remains as to whether it is correlated along the length of the cylinder.

Removing the narrow band and deterministic flow features such as vortex shedding and duct acoustic and room resonances it was found that the correlation length was small as noted above. This would suggest that the jet switching was not correlated along the length of the cylinder. Figure 14 presents the time resolved pressure signals at a position angle of θ=250^o, a velocity of 7m/s and a number of spanwise positions. It is observed that the jet switching can vary over the length of the cylinder. At some angular positions and flow velocities tested it is clear that the jet switching is well correlated along the cylinder. Clearly there is a disparity between the calculated correlation coefficient which is low and the raw pressure data showing the opposite with high correlation. This is due to the fact the jet switching is a high frequency process but a low occurrence phenomenon. For example, the jet switches from one mode to another mode nearly instantaneously but the duration at each mode is random; in one instance it was 3 seconds in another instance it was 15 seconds. It is envisaged that if very long time record was used there would be agreement between the calculated correlation and that observed from the pressure signals.

In addition there appears to be some interesting behaviour in flow. Examining the pressure signals at z/d=1.66 and 0.47; and z/d=-1.89 it appears that there are striations or cells in the flow structure. It is not clear why this is the case and this requires further analysis.

It is reported in the literature (1; 2; 3) that the correlation length is small (typically $<$ one diameter). This is consistent with the results presented in the current study for both pitch ratios. It is important to note that correlation length is small for turbulent buffeting forces as was the case for P/d=1.32 where no jet switching was observed. However, if jet switching is observed, as was the case in the pitch ratio of 1.58 it maybe incorrect to assume the correlation length is small. This result brings into question one of the key assumptions in the models (Axisa *et al.* (1) and Pettigrew & Taylor (14)) to predict the random buffeting forces on a cylinder. In fact, the results presented highlight the need to consider jet switching when calculating fretting wear as without the inclusion of jet switching in the models the life cycle of components subject to random turbulent forces and jet switching may be significantly overestimated.

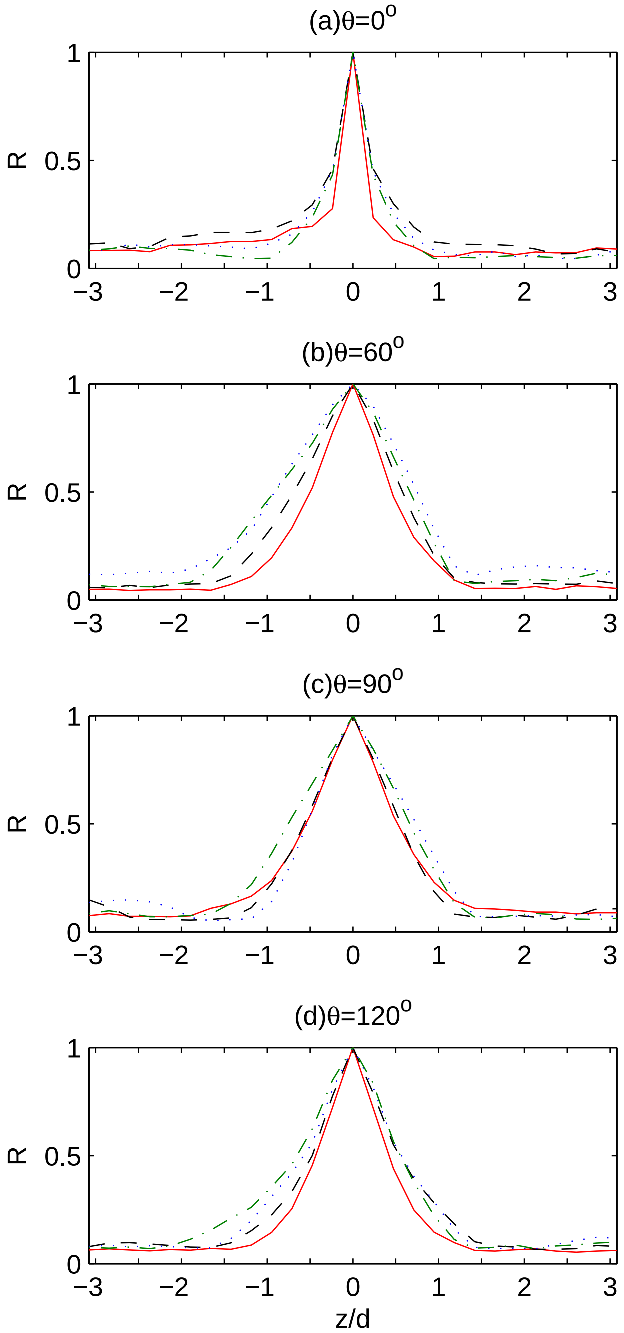

FIGURE 11. Spanwise correlation at a range of angular positions; P/d=1.58; —, U_g=8.2m/s; — —, U_g=19.1m/s; · · ·, U_g=30.0m/s; — · —, U_g=38.2m/s

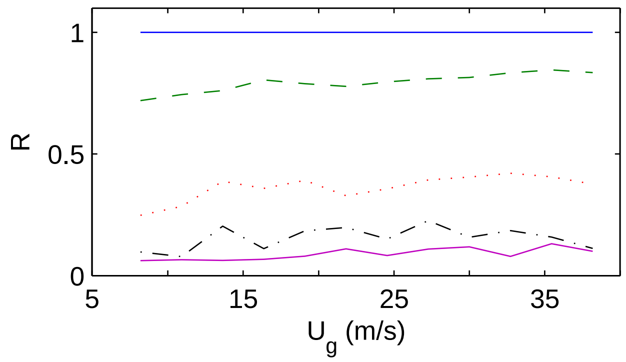

FIGURE 12. Spanwise correlation at different velocities; P/d=1.58, θ=120^o; —, z/d=0; — —, z/d=0.24; · · ·, z/d=0.71; — · —, z/d=1.66; —, z/d=3.08

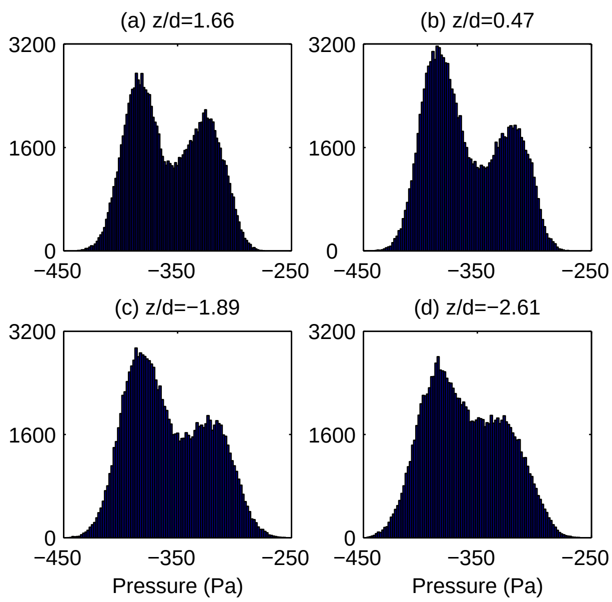

FIGURE 13. Histogram of pressure signals at θ=250^o; 1.58; z/d=1.66, z/d=0.47, z/d=-1.89 and z/d=-2.61

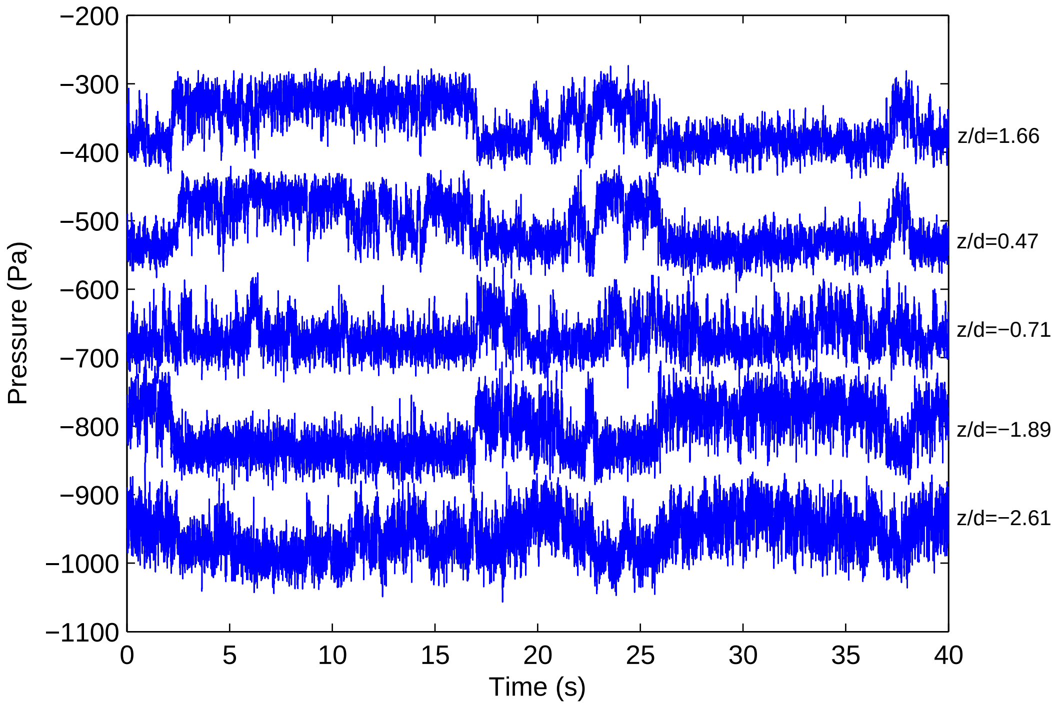

FIGURE 14. Time resolved pressure signals at θ=250^o; 1.58; z/d=1.66, z/d=0.47, z/d=-0.71, z/d=-1.89 and z/d=-2.61

CONCLUSIONS

An experimental study of the surface spanwise pressure on a cylinder in the third row of two normal triangular tube arrays (P/d=1.32 and 1.58) with air cross flow has been conducted. The correlation of turbulent buffeting forces along the length of the cylinder is small and is in agreement with the literature. However, vortex shedding and acoustic resonance are well correlated. Jet switching was observed in the pitch ratio of 1.58 and was correlated along the cylinder. This result suggests that the models used to predict fretting wear may need to be modified to include jet switching, as a spanwise correlated excitation which has broadband content will act as an efficient excitation mechanism in the lightly damped structures typical of heat exchangers.

ACKNOWLEDGMENT

This publication has emanated from research conducted with the financial support of Science Foundation Ireland.

REFERENCES

[1] Axisa, F., Antunes, J., and Villard, B., 1990. "Random excitation of heat exchanger tubes by cross-flows". *Journal of Fluids and Structures,* ***4***, pp. 321–241.

[2] Batham, J. P., 1973. "Pressure distributions on circular cylinders at critical reynolds numbers". *Journal of Fluid Mechanics,* ***57***(2), pp. 209–228.

[3] Romberg, O., and Popp, K., 1999. "Fluid damping controlled instability in tube bundles subjected to air crossflow". *Flow, Turbulence and Combustion,* ***61***, pp. 285–300.

[4] Mahon, J., and Meskell, C., 2009. "Surface pressure distribution survey in normal triangular tube arrays". *Journal of Fluids and Structures,* ***25***, pp. 1348–1368.

[5] Oengoren, A., and Ziada, S., 1995. "Vortex shedding, acoustic resonance and turbulent buffeting in normal triangular tube arrays". *P Bearman (Ed.), Flow-Induced Vibration,* ***Balkema***, pp. 295–313.

[6] Zukauskas, A. A., and Katinas, V. J. "Flow-induced vibration in heat exchanger tube banks". *Proceedings of the IUTAM IAHR symposium on practical experiences with flow-induced vibrations, Karlsruhe, 1979, eds., Naudascher, E., Rockwell, D. Springer-Verlag, Berlin*.

[7] Weaver, D. S., Fitzpatrick, J. A., and El-Kashlan, M., 1986. "Strouhal numbers for heat exchanger tube arrays in cross flow". *In: S.S. Chen, J.C. Simonis and Y.S. Shin, Editors, Flow-Induced Vibration, ASME Publication PVP-104, ASME, New York (1986),* ***104***(2), pp. 193–200.

[8] Blevins, R. D., and Bressler, M. M., 1987. "Acoustic resonance in heat exchanger tube bundles-part 1: Physical nature of the phenomenon; part ii: Prediction and suppression of resonance". *ASME Journal of Pressure Vessel Technology,* ***109***, pp. 275–288.

[9] Hill, R, S. K. C., and Lewis, R. I., 1986. "Sources of excitation in tube banks due to vortex shedding". *Proceedings of Institute of Mechanical Engineers,* ***200***(C4), pp. 293–301.

[10] Pettigrew, M. J., and Gorman, D. J., 1978. "Vibration of heat exchange components in liquid and two-phase cross-flow". *International Conference Vibration in Nuclear Plant, Kewswick, U.K.,* ***2***(2.3).

[11] Polak, D., and Weaver, D. S., 1995. "Vortex shedding in normal triangular tube arrays". *Journal of Fluids and Structures,* ***9***, pp. 1–17.

[12] Price, S. J., and Zahn, M. L., 1991. "Fluidelastic behaviour of a normal triangular array subject to cross-flow". *Journal of Fluids and Structures,* ***5***, pp. 259–278.

[13] Weaver, D. S., and Yeung, H. C., 1984. "The effect of tube mass on the flow induced response of various tube arrays in water". *Journal of Sound and Vibration,* ***93***(3), pp. 409–425.

[14] Pettigrew, M. J., and Taylor, C. E., 2003. "Vibration analysis of shell-and-tube heat exchangers: an overview - part 2: vibration response, fretting-wear, guidelines". *Journal of Fluids and Structures,* ***18***, pp. 485–500.